

Study of the alpha-particle monopole transition form factor

M. Viviani^{1*}, A. Kievsky¹, L.E. Marcucci^{2,1}, L. Girlanda^{3,4}

¹*Sezione di Pisa, Istituto Nazionale di Fisica Nucleare, Largo B. Pontecorvo 3, Pisa, I-56127, Italy.

²Department of Physics “E. Fermi”, University of Pisa, Largo B. Pontecorvo 3, Pisa, I-56127, Italy.

³Department of Mathematics and Physics, University of Salento, Via Arnesano, Lecce, I-73100, Italy.

⁴Sezione di Lecce, Istituto Nazionale di Fisica Nucleare, Via Arnesano, Lecce, I-73100, Italy.

*Corresponding author(s). E-mail(s): michele.viviani@pi.infn.it;
Contributing authors: alejandro.kievsky@pi.infn.it;
laura.elisa.marcucci@unipi.it; girlanda@le.infn.it;

Abstract

The ${}^4\text{He}$ monopole form factor is studied by computing the transition matrix element of the electromagnetic charge operator between the ${}^4\text{He}$ ground-state and the $p + {}^3\text{H}$ and $n + {}^3\text{He}$ scattering states. The nuclear wave functions are calculated using the hyperspherical harmonic method, by starting from Hamiltonians including two- and three-body forces derived in chiral effective field theory. The electromagnetic charge operator retains, beyond the leading order (impulse approximation) term, also higher order contributions, as relativistic corrections and meson-exchange currents. The results for the monopole form factor are in fairly agreement with recent MAMI data. Comparison with other theoretical calculations are also provided.

1 Introduction

The ${}^4\text{He}$ nucleus is a fundamental system for our comprehension of nuclear forces. The four nucleons form a ground state of quantum numbers $J^\pi = 0^+$, hereafter denoted

as the 0_0^+ state. Such a state is rather deeply bound, with a binding energy of about 7 MeV per nucleon. In addition, the ^4He nucleus has also a number of excited states, which, however, are not true bound states but resonances. The first excited state 0_1^+ (which has the same quantum numbers as the ground state) is, in fact, unstable for the splitting in the $p + ^3\text{H}$ subsystems. It lies approximately 20 MeV above the ground state, but below the opening of the $n + ^3\text{He}$ channel [1]. Clearly, for the description of this resonance, the Coulomb interaction plays a very important role [2].

The nature of such a resonance is still a puzzle after many years of studies [3]. The process $^4\text{He}(e, e')X$ can be used to obtain direct information on the monopole form factor $F_M(q)$ (which is essentially the matrix element of the electromagnetic transition operator between the initial and final states), detecting scattered electrons which have lost approximately 20 MeV of energy. The experiments performed in the past [4–6] could not achieve a great accuracy. However, more recently, an experiment performed at the Mainz Microtron (MAMI) allowed to extract quite accurate data for $F_M(q)$ [7]. In this experiment, electron beams with energies of 450, 690, and 795 MeV were directed onto a target consisting of cryogenic helium gas. The scattered electrons were detected using a sophisticated apparatus, which allowed to observe both the elastic peak and the first-excited state resonance. The ^4He elastic peak was used to determine quite accurately the luminosity and to estimate the experimental resolution needed for the precise extraction of the monopole form factor (however, a careful analysis of the data is necessary in order to subtract the non-resonant contributions, see Ref. [7] for more details).

In the past years, several theoretical studies of $F_M(q)$ were also performed. In Ref. [8], $F_M(q)$ was calculated using a bound state technique, expanding the wave functions over a Gaussian basis. The result of this calculation is in good agreement with both the old and the MAMI experimental data. In Refs. [7, 9, 10], a calculation using the Lorentz Integral Transform (LIT) method to sum implicitly all the intermediate states was performed. In this case, the calculated monopole form factor was found to be rather at variance with respect to the experimental data, in particular with respect to the precise MAMI data [7]. More recently, a calculation performed using the no-core Gamow shell model method, including explicit $p + ^3\text{H}$, $n + ^3\text{He}$, and $d + d$ reaction channels, allows to reproduce the MAMI data [11]. A similar conclusion was found in another recent calculation performed in the framework of nuclear lattice effective field theory [12].

These calculations were performed using different Hamiltonians. In Ref. [8], the results were obtained using the Argonne V8 (AV8') [14] nucleon-nucleon (NN) potential plus a simple three-nucleon (3N) interaction. The calculations of Refs. [7, 9, 10] were performed using a NN+3N interaction derived within the framework of the chiral effective field theory (χEFT). The Hamiltonian used in the calculation of Ref. [11] is based on the V_{low-k} version of the same NN interaction used in Refs. [7, 9, 10], adopting the cutoff value $\Lambda = 1.9 \text{ fm}^{-1}$ [13], but without including any 3N force. Finally, in the calculation performed in the framework of nuclear lattice effective field theory [12], a rather simple nuclear interaction has been used, in practice containing NN+3N contact terms. Anyway, this interaction is capable of reproducing the ground state properties

of light nuclei, medium-mass nuclei, and neutron matter simultaneously with no more than a few percent error in the energies and charge radii [12].

In order to analyse further this process, we have reconsidered the study of the monopole transition form factor, exploiting our expertise in the calculation of four-nucleon (4N) scattering wave functions. Using modern realistic Hamiltonians we have computed the transition matrix element between the ${}^4\text{He}$ ground-state and the $p + {}^3\text{H}$ and $n + {}^3\text{He}$ scattering states including in the transition operator terms beyond the leading order (impulse approximation), as relativistic corrections and meson-exchange contributions. This calculation follows somewhat the experimental technique itself, where the electrons scatters the ${}^4\text{He}$ nuclei, producing final states composed by different clusters as $p + {}^3\text{H}$, $n + {}^3\text{He}$, etc. To compute $F_M(q)$ we have to integrate over the possible final states of different energies produced in the process.

We have performed this study using the NN chiral interaction derived at next-to-next-to-next-to-leading order (N3LO) by Entem and Machleidt [15, 16], with cutoffs $\Lambda = 500, 600$ MeV. We have also performed calculations including the chiral 3N interaction derived at next-to-next-to leading order (N2LO) in Refs. [17, 18]. The two free parameters in this N2LO 3N potential, denoted usually as c_D and c_E , have been fixed in order to reproduce the experimental values of the $A = 3$ binding energies and the Gamow-Teller matrix element of the tritium β decay [19, 20]. Note that these parameters have been recently redetermined [21–23].

The 4N wave functions are calculated using the so-called hyperspherical harmonics (HH) technique [24, 25]. Several benchmarks performed in the past have shown the good accuracy which can be achieved by this method for both the 4N bound state problem [26, 27] and the 4N scattering problem [28, 29]. The detailed application of the HH method to the 4N scattering problem is reported in Ref. [30], where the convergence issues are throughout discussed and several results for $n + {}^3\text{H}$, $p + {}^3\text{He}$, $p + {}^3\text{H}$, and $n + {}^3\text{He}$ scattering are given.

This paper is organized as follows. In Section 2, a description of the HH method for bound and scattering states is briefly resumed, and the approach for calculating $F_M(q)$ is presented. The results are given in Section 3, where the comparison with the experimental data and the results of other theoretical calculations is reported. The conclusions and the perspectives of this work will be given in Section 4.

2 Theoretical formalism

This section is divided into three subsections. In the first two, we briefly introduce the HH method to compute 4N bound and scattering states. In the last subsection we present the approach employed to calculate $F_M(q)$.

2.1 The HH method

We start with the definition of the Jacobi vectors which, for a system of four identical particles (disregarding the proton-neutron mass difference), are given by

$$\boldsymbol{\xi}_{1p} = \sqrt{\frac{3}{2}} \left(\mathbf{r}_l - \frac{\mathbf{r}_i + \mathbf{r}_j + \mathbf{r}_k}{3} \right),$$

$$\begin{aligned}\boldsymbol{\xi}_{2p} &= \sqrt{\frac{4}{3}} \left(\mathbf{r}_k - \frac{\mathbf{r}_i + \mathbf{r}_j}{2} \right), \\ \boldsymbol{\xi}_{3p} &= \mathbf{r}_j - \mathbf{r}_i,\end{aligned}\tag{1}$$

where p specifies a permutation corresponding to the order i, j, k and l of the particles. By definition, the permutation $p = 1$ is chosen to correspond to the order 1, 2, 3 and 4. In terms of the Jacobi vectors, the kinetic energy T is written as

$$T = -\frac{1}{M} \left(\nabla_{\boldsymbol{\xi}_{1p}}^2 + \nabla_{\boldsymbol{\xi}_{2p}}^2 + \nabla_{\boldsymbol{\xi}_{3p}}^2 \right),\tag{2}$$

where M is the nucleon mass (hereafter $\hbar = c = 1$). For a given choice of the Jacobi vectors, the hyperspherical coordinates are given by the so-called hyperradius ρ , defined by

$$\rho = \sqrt{\xi_{1p}^2 + \xi_{2p}^2 + \xi_{3p}^2}, \quad (\text{independent of } p),\tag{3}$$

and by a set of angular variables which in the Zernike and Brinkman [31, 32] representation are (i) the polar angles $\hat{\boldsymbol{\xi}}_{ip} \equiv (\theta_{ip}, \phi_{ip})$ of each Jacobi vector, and (ii) two additional angles, called hyperangles, φ_{2p} and φ_{3p} defined as

$$\cos \varphi_{2p} = \frac{\xi_{2p}}{\sqrt{\xi_{1p}^2 + \xi_{2p}^2}}, \quad \cos \varphi_{3p} = \frac{\xi_{3p}}{\sqrt{\xi_{1p}^2 + \xi_{2p}^2 + \xi_{3p}^2}},\tag{4}$$

where ξ_{jp} is the modulus of the Jacobi vector $\boldsymbol{\xi}_{jp}$. The set of angular variables $\hat{\boldsymbol{\xi}}_{1p}, \hat{\boldsymbol{\xi}}_{2p}, \hat{\boldsymbol{\xi}}_{3p}, \varphi_{2p}, \varphi_{3p}$ is denoted hereafter as Ω_p . The expression of a generic HH function is

$$\begin{aligned}\mathcal{H}_{\ell_1, \ell_2, \ell_3, L_2, n_2, n_3}^{K, \Lambda, M}(\Omega_p) &= \\ &\mathcal{N}_{n_2, n_3}^{\ell_1, \ell_2, \ell_3} \left[\left(Y_{\ell_1}(\hat{\boldsymbol{\xi}}_{1p}) Y_{\ell_2}(\hat{\boldsymbol{\xi}}_{2p}) \right)_{L_2} Y_{\ell_3}(\hat{\boldsymbol{\xi}}_{3p}) \right]_{\Lambda M} \\ &\times (\sin \varphi_{2p})^{\ell_1} (\cos \varphi_{2p})^{\ell_2} P_{n_2}^{\ell_1 + \frac{1}{2}, \ell_2 + \frac{1}{2}}(\cos 2\varphi_{2p}) \\ &\times (\sin \varphi_{3p})^{\ell_1 + \ell_2 + 2n_2} (\cos \varphi_{3p})^{\ell_3} P_{n_3}^{\ell_1 + \ell_2 + 2n_2 + 2, \ell_3 + \frac{1}{2}}(\cos 2\varphi_{3p}),\end{aligned}\tag{5}$$

where $P_n^{a,b}$ are Jacobi polynomials and the coefficients $\mathcal{N}_{n_2, n_3}^{\ell_1, \ell_2, \ell_3}$ normalization factors. The quantity $K = \ell_1 + \ell_2 + \ell_3 + 2(n_2 + n_3)$ is the grand angular quantum number. The HH functions are the eigenfunctions of the hyperangular part of the kinetic energy operator. Furthermore, $\rho^K \mathcal{H}_{\ell_1, \ell_2, \ell_3, L_2, n_2, n_3}^{K, \Lambda, M}(\Omega_p)$ are homogeneous polynomials of the particle coordinates of degree K .

A set of antisymmetric hyperangular–spin–isospin states of grand angular quantum number K , total orbital angular momentum Λ , total spin Σ , and total isospin T (for

given values of total angular momentum J and parity π) can be constructed as follows:

$$\Psi_\mu^{K\Lambda\Sigma T} = \sum_{p=1}^{12} \Phi_\mu^{K\Lambda\Sigma T}(i, j, k, l), \quad (6)$$

where the sum is over the 12 even permutations $p \equiv i, j, k, l$, and

$$\Phi_\mu^{K\Lambda\Sigma T}(i, j, k; l) = \left\{ \mathcal{H}_{\ell_1, \ell_2, \ell_3, L_2, n_2, n_3}^{K, \Lambda}(\Omega_p) \left[\left[(s_i s_j)_{S_a} s_k \right]_{S_b} s_l \right]_{\Sigma} \right\}_{JJ_z} \left[\left[(t_i t_j)_{T_a} t_k \right]_{T_b} t_l \right]_{TT_z}. \quad (7)$$

Here, $\mathcal{H}_{\ell_1, \ell_2, \ell_3, L_2, n_2, n_3}^{K, \Lambda}(\Omega_p)$ is the HH state defined in Eq. (5), and s_i (t_i) denotes the spin (isospin) function of particle i . The total orbital angular momentum Λ of the HH function is coupled to the total spin Σ to give the total angular momentum JJ_z , whereas $\pi = (-1)^{\ell_1 + \ell_2 + \ell_3}$. The quantum number T specifies the total isospin of the state. The integer index μ labels the possible choices of hyperangular, spin and isospin quantum numbers, namely

$$\mu \equiv \{\ell_1, \ell_2, \ell_3, L_2, n_2, n_3, S_a, S_b, T_a, T_b\}, \quad (8)$$

compatibles with the given values of K, Λ, Σ, T, J and π . Each state $\Psi_\mu^{K\Lambda\Sigma T}$ entering the expansion of the 4N wave function must be antisymmetric under the exchange of any pair of particles. To this aim it is sufficient to consider states such that

$$\Phi_\mu^{K\Lambda\Sigma T}(i, j, k; l) = -\Phi_\mu^{K\Lambda\Sigma T}(j, i, k; l), \quad (9)$$

which is fulfilled when the condition

$$\ell_3 + S_a + T_a = \text{odd}, \quad (10)$$

is satisfied. Note that many of the antisymmetric states $\Psi_\mu^{K\Lambda\Sigma T}$ are linearly dependent between themselves.

The 4N wave function can be finally written as

$$\Psi_C = \sum_{K\Lambda\Sigma T} \sum_{\mu} u_{K\Lambda\Sigma T\mu}(\rho) \Psi_\mu^{K\Lambda\Sigma T}, \quad (11)$$

where the sum is restricted only to the linearly independent states. This expansion can be used to compute either a bound-state wave function or the ‘‘internal’’ part of the scattering wave function (see next subsection). We have found convenient to expand the hyperradial functions $u_{K\Lambda\Sigma T\mu}(\rho)$ in a complete set of functions, namely

$$u_{K\Lambda\Sigma T\mu}(\rho) = \sum_{m=0}^{M-1} c_{K\Lambda\Sigma T\mu m} g_m(\rho), \quad (12)$$

and we have chosen

$$g_m(\rho) = \sqrt{b^9 \frac{m!}{(m+8)!}} L_m^{(8)}(b\rho) e^{-\frac{b}{2}\rho}, \quad (13)$$

where $L_m^{(8)}(b\rho)$ are Laguerre polynomials [33] and b is a parameter to be variationally optimized.

One of the problem we have to face is that the number of linearly independent states is still very high, and increases noticeably with K . In order to reduce the number of states to be included in the expansion, we adopt the same strategy as described in Refs. [27, 30]. Namely, we divide the basis in classes, depending on the value of the quantity $\mathcal{L} = \ell_1 + \ell_2 + \ell_3$ and the values of n_2, n_3 , see Section 3 of Ref. [27] for the detailed definition of the classes. Hereafter, we consider only the definition of the classes of HH functions for the state having total angular momentum and parity $J^\pi = 0^+$ and total isospin $T = 0$, which is the case we are interested in. In fact, in the present work, we can safely disregard HH states with $T > 0$.

Briefly, the first two classes include the states with $\mathcal{L} = 0$ and a selected set of states with $\mathcal{L} = 2$, the third class the remaining states with $\mathcal{L} = 2$ and the fourth and the fifth classes the states with $\mathcal{L} = 4$ and $\mathcal{L} = 6$, respectively. We have found that the convergence of the various quantities depends critically on the value of \mathcal{L} . Classes with low values of \mathcal{L} , typically $\mathcal{L} = 0, 2$, require the inclusion of HH states with large values of K whereas this is not the case for higher values of \mathcal{L} . The contributions of the fourth and fifth classes to either the binding energy or to scattering observables becomes smaller and smaller as K is increased, in particular the contribution of the fifth class is practically negligible. This is due to the fact that states with large values of \mathcal{L} suffer for a high centrifugal barrier describing with a low probability particles close to each other. This reduces the importance of the corresponding HH states (we remember that the nuclear force is short range). In the following, we report the results obtained using different basis sets of HH functions, each of one corresponding to different values of K_α , $\alpha = 1, 5$. These values specify that in the class α , only states of grand angular quantum number $K \leq K_\alpha$ are included. The values adopted in the present work are given in Table 1, together with the total number of HH functions included in the expansion.

The ground state is calculated using the expansion given in Eq.(11), and expanding the hyperradial functions as in Eq.(12). In order to describe with great accuracy this state the values of K_α given in the upper part of Table 1 can be used. For the scattering state, the function given in Eq. (11) is used to describe the internal part of the wave function, namely the region where all the four nucleons are close to each other (the full wave function will be detailed in the next subsection). In this case the expansion has to describe the transition between the internal region and the asymptotic region in which the clusters are well separated with the consequence that one needs to increase K_{1-5} . For both the ground state and the scattering states, we provide three basis sets with increasing values of K_α , see Table 1. The various basis sets will be used in Sect. 3 to check the convergence of the results.

Table 1 Different basis sets of HH functions used in this calculation. Each basis set is specified by giving the maximum grand angular quantum numbers for the various classes of HH states included in Ψ_C . The value of K_α for the class α means that we have included all HH functions with $K \leq K_\alpha$ (for the definition of the classes, see Refs. [27, 30]).

For the ground state						
set	K_1	K_2	K_3	K_4	K_5	N
A1	28	20	20	20	0	2,498
A2	30	22	22	22	0	3,145
A3	32	24	24	24	0	3,871
For the scattering states						
set	K_1	K_2	K_3	K_4	K_5	N
B1	46	42	32	40	20	7,548
B2	48	44	34	42	22	8,838
B3	50	46	36	44	24	10,053

2.2 The scattering wave function

In the following, a specific clusterization $A + B$ will be denoted by the index γ . More specifically, $\gamma = 1$ (2) stands for the clusterization $p + {}^3\text{H}$ ($n + {}^3\text{He}$). Let us consider a scattering state with total angular momentum quantum number JJ_z , and parity π . Here, we are interested only on the case where $J^\pi = 0^+$, so in the following these values are understood. The wave function $\Psi^{\gamma LS}$ describing incoming clusters γ with relative orbital angular momentum L and channel spin S , coupled to JJ_z , can be written as

$$\Psi^{\gamma LS} = \Psi_C^{\gamma LS} + \Psi_A^{\gamma LS}, \quad (14)$$

where the core part $\Psi_C^{\gamma LS}$ describes the four particles when they are close to each other; it can be conveniently expanded as in Eq. (11). The other term, $\Psi_A^{\gamma LS}$, describes the relative motion of the two clusters in the asymptotic regions, where the mutual interaction is negligible (except for the long-range Coulomb interaction), and it can be decomposed as a linear combination of the following functions

$$\Omega_{\gamma LS}^F = \frac{1}{\sqrt{4}} \mathcal{A} \left\{ \left[Y_L(\hat{\boldsymbol{y}}_\gamma) [\Phi_\gamma(ijk)_{si}]_S \right]_{JJ_z} \frac{F_L(\eta_\gamma, q_\gamma y_\gamma)}{q_\gamma y_\gamma} \right\}, \quad (15)$$

$$\Omega_{\gamma LS}^G = \frac{1}{\sqrt{4}} \mathcal{A} \left\{ \left[Y_L(\hat{\boldsymbol{y}}_\gamma) [\Phi_\gamma(ijk)_{si}]_S \right]_{JJ_z} \frac{G_L(\eta_\gamma, q_\gamma y_\gamma)}{q_\gamma y_\gamma} (1 - e^{-\beta y_\gamma})^{2L+1} \right\}, \quad (16)$$

where y_γ is the distance between the center-of-mass (c.m.) of clusters A and B , q_γ is the magnitude of the relative momentum between the two clusters, and $\Phi_\gamma(ijk)$ are the bound state wave functions (clearly, $\Phi_1 \equiv \Phi_{3\text{H}}$ and $\Phi_2 \equiv \Phi_{3\text{He}}$). In the present work, the trinucleon bound state wave functions $\Phi_\gamma(ijk)$ (for both ${}^3\text{He}$ and ${}^3\text{H}$) are described using the HH method [24, 34]. Moreover, the channel spin S is obtained coupling the angular momentum of the two clusters. In our case, we have

$S = 0, 1$. The symbol \mathcal{A} means that the expression between the curly braces has to be properly antisymmetrized, summing over the permutations of the particles $(ijk), l$ with $l = 1, \dots, 4$ ($\Phi_\gamma(ijk)$ are already antisymmetric under the exchange of ijk).

The c.m. kinetic energy E_γ in the channel γ is defined by the relations

$$E_T = -B(^3\text{H}) + E_1 = -B(^3\text{He}) + E_2 \quad (17)$$

where E_T is the c.m. energy of the state and $B(^3\text{H})$ and $B(^3\text{He})$ the binding energies of ^3H and ^3He , respectively. Depending on the value of E_T , E_γ can be either positive or negative. In the present paper, we are interested in the range of energies $-B(^3\text{H}) \leq E_T \leq -2B(d)$, where $B(d)$ is the deuteron binding energy. Namely, we are below the opening of the $d + d$ channel. When $E_\gamma > 0$, the wave number q_γ is defined as

$$E_\gamma = \frac{q_\gamma^2}{2\mu_\gamma}, \quad \frac{1}{\mu_\gamma} = \frac{1}{M_A} + \frac{1}{M_B}, \quad (18)$$

and M_X is the mass of the cluster X . Clearly, in the case of a single nucleon $M_X = M$. In the present case E_1 is always positive, while $E_2 < 0$ for $-B(^3\text{H}) \leq E_T \leq -B(^3\text{He})$ (see below to see how this case has been treated).

In Eqs. (15) and (16), the functions F_L and G_L describe the asymptotic radial motion of the clusters A and B . If the two clusters are composed of Z_A and Z_B protons, respectively, the parameter η_γ is defined as $\eta_\gamma = \mu_\gamma Z_A Z_B e^2 / q_\gamma$, where $e^2 = 1.43997$ MeV fm. The functions $F_L(\eta, qy)$ and $G_L(\eta, qy)$ are the regular and irregular Coulomb function, respectively. The term $(1 - e^{-\beta y_\gamma})^{2L+1}$ is used to “regularize” the irregular Coulomb function for $y_\gamma \rightarrow 0$ (see Ref. [30] for more details), but it does not affect the long range behavior. The parameter β is usually chosen to be $\beta = 0.25$ fm $^{-1}$. Let us also define

$$\Omega_{\gamma LS}^\pm = \Omega_{\gamma LS}^G \pm i\Omega_{\gamma LS}^F, \quad (19)$$

where $\Omega_{\gamma LS}^+$ ($\Omega_{\gamma LS}^-$) describes the outgoing (ingoing) relative motion of the clusters specified by γ . In fact, their asymptotic behaviour is described as

$$G_L(\eta, qy) \pm iF_L(\eta, qy) \rightarrow e^{\pm i(qy - L\pi/2 - \eta \ln(2qy) + \sigma_L)}, \quad (20)$$

where σ_L is the Coulomb phase shift.

If one of the clusters is a neutron (case $\gamma = 2$), then $\eta = 0$ and the functions F_L and G_L reduce to

$$\frac{F_L(\eta, qy)}{qy} \rightarrow j_L(qy), \quad \frac{G_L(\eta, qy)}{qy} \rightarrow -y_L(qy), \quad (21)$$

where j_L and y_L are the regular and irregular spherical Bessel functions defined, for example, in Ref. [33]. Finally, the general expression of $\Psi_A^{\gamma LS}$ entering Eq. (14) is

$$\Psi_A^{\gamma, L, S} = \Omega_{\gamma, L, S}^F + \sum_{\gamma', L', S'} \mathcal{T}_{L, S; L', S'}^{\gamma, \gamma'} \Omega_{\gamma', L', S'}^+, \quad (22)$$

where the parameters $\mathcal{T}_{LS,L'S'}^{\gamma,\gamma'}$ are the so-called T -matrix elements. Of course, the sum over L' and S' is over all values compatible with the given J and parity π . In the present case, with $J^\pi = 0^+$, we have simply $L, S = L', S' = 0, 0$.

Limiting ourselves to energies below the opening of the $d + d$ channels, the $p + {}^3\text{H}$ scattering wave function in the 0^+ state is given by

$$\Psi^{1,0,0}(E_1) = \Psi_C^{1,0,0} + \Omega_{1,0,0}^F + \mathcal{T}_{0,0;0,0}^{1,1}\Omega_{1,0,0}^+ + \mathcal{T}_{0,0;0,0}^{1,2}\Omega_{2,0,0}^+. \quad (23)$$

Here we have included the term $\Omega_{2,0,0}^+$ below the $n + {}^3\text{He}$ threshold even if the channel is energetically “closed” (namely the energy E_2 , fixed by the relation $E_T = -B_{^3\text{He}} + E_2$, is such that $E_2 < 0$). In this case $q_2 = i\alpha_2$, where $\alpha_2 = \sqrt{2\mu_2|E_2|}$, and $\Omega_{2,0,0}^+$ reduces to

$$\Omega_{2,0,0}^+ = \frac{1}{\sqrt{4}}\mathcal{A}\left\{ \left[Y_0(\hat{\mathbf{y}}_\gamma)[\Phi_2(ijk)_{sl}]_0 \right]_{0,0} \frac{e^{-\alpha_2 y_2}}{y_2} (1 - e^{-\beta y_2}) \right\}. \quad (24)$$

From a computational point of view, the presence of this term below the $n + {}^3\text{He}$ threshold is very useful. In fact, as $E_T \rightarrow -B({}^3\text{He})$ (from below), α_2 becomes rather small and the component $\Omega_{2,0,0}^+$ will have a long-range tail, in spite of the exponential term $e^{-\alpha_2 y_2}$. Configurations of this type are rather difficult to be constructed in terms of the “internal” part Ψ_C . Therefore, including this term in the variational wave function is decisive in order to solve the convergence problem found for $p + {}^3\text{H}$ scattering in Ref. [30] below the $n + {}^3\text{He}$ threshold.

Above the $n + {}^3\text{He}$ threshold, we have to consider also the wave function with the term $\Omega_{2,0,0}^F$, namely

$$\Psi^{2,0,0}(E_2) = \Psi_C^{2,0,0} + \Omega_{2,0,0}^F + \mathcal{T}_{0,0;0,0}^{2,1}\Omega_{1,0,0}^+ + \mathcal{T}_{0,0;0,0}^{2,2}\Omega_{2,0,0}^+. \quad (25)$$

We remember that the relation between E_1 and E_2 is given in Eq. (17).

2.3 The monopole form factor

As discussed in the Introduction, the monopole form factor is extracted from the $e + {}^4\text{He}$ cross section. Below the $n + {}^3\text{He}$ threshold, the process to be considered is ${}^4\text{He}(e, e'p){}^3\text{H}$, while above that threshold, the contribution of the process ${}^4\text{He}(e, e'n){}^3\text{He}$ has also to be considered. However, for the sake of simplicity, in the present subsection we work out the cross section for the ${}^4\text{He}(e, e'p){}^3\text{H}$ process only, giving the complete expression of $F_M(q)$ at the end. In any case, we restrict our study to energies below the $d + d$ threshold.

In the following \mathbf{k} and s (\mathbf{k}' and s') are the momentum and spin projection of the incoming (outgoing) electron. The ${}^4\text{He}$ is considered at rest, while the final proton (${}^3\text{H}$) has momentum \mathbf{p}_1 (\mathbf{p}_3) and spin projection m_1 (m_3). Clearly $\mathbf{q} = \mathbf{k} - \mathbf{k}'$ and $\omega = k - k'$ are the momentum and energy transfer. The electrons are ultrarelativistic, hence we will consider them as massless. For example, in the MAMI experiment, the incident beam energy was in the range 430-780 MeV. As discussed above, $\omega \approx 20$ MeV, so also the final electrons can be safely considered as ultrarelativistic.

The cross section can be calculated using the Fermi Golden Rule

$$d\sigma = \frac{1}{2} \sum_{ss'} \sum_{m_1, m_3} \sum_{\mathbf{k}', \mathbf{p}_1, \mathbf{p}_3} 2\pi\delta(E_i - E_f) |T_{fi}|^2 \delta_{\mathbf{k}, \mathbf{k}' + \mathbf{p}_1 + \mathbf{p}_3}, \quad (26)$$

where $E_i = k + M_4$ and

$$E_f = k' + M_3 + \frac{\mathbf{p}_3^2}{2M_3} + M + \frac{\mathbf{p}_1^2}{2M}, \quad (27)$$

M , M_3 , and M_4 being the nucleon, ^3H , and ^4He masses, respectively. In the previous expression, we can safely use the non relativistic expression for the proton and ^3H kinetic energies. The transition matrix element T_{fi} is given by

$$T_{fi} = 4\pi\alpha \frac{H^\mu \ell_\mu}{(-Q^2)}, \quad (28)$$

where H^μ and ℓ^μ are the hadronic and leptonic matrix elements, respectively, and $Q^2 = q^2 - \omega^2$. Above, α is the fine structure constant, $\alpha \approx 1/137$. The hadronic matrix element is decomposed as usual in multipoles. We are interested to the transition $0_0^+ \rightarrow 0_1^+$ induced by the electron scattering, therefore, we only need to compute the matrix element of the charge operator $\hat{\rho}(\mathbf{q})$, which at leading order (or in impulse approximation) is simply given by

$$\hat{\rho}(\mathbf{q}) = \sum_{j=1}^4 f_p(q) \frac{1 + \tau_z(j)}{2} e^{i\mathbf{q} \cdot \mathbf{r}_j}, \quad (29)$$

where $f_p(q)$ is the proton form factor chosen to be [35]

$$f_p(q) = \frac{1}{(1 + 0.056 q^2)^2}, \quad (30)$$

q being given in fm^{-1} . In principle, the proton form factor should depend on Q , with $Q^2 = q^2 - \omega^2$, ω being the energy transfer. However, in the process under consideration $\omega \approx 20$ MeV, while the typical values of q are of the order of $1 \text{ fm}^{-1} \approx 200$ MeV, so we can safely neglect ω^2 with respect to q^2 .

In the calculation, we will consider also the contribution of various corrections to the operator given in Eq. (29), as relativistic corrections and meson-exchange terms, derived within χEFT [36]. As we will see, these latter contributions are small but sizable, in particular for large values of q . The wave function of the final $p + ^3\text{H}$ state can be written as

$$\begin{aligned} \Psi_{m_3, m_1}^{1+3}(\mathbf{p}) = & \sum_{SS_z LM JJ_z} \left(\frac{1}{2}, m_3, \frac{1}{2}, m_1 | S, S_z\right) (L, M, S, S_z | J, J_z) \\ & \times 4\pi i^L e^{i\sigma_L} Y_{LM}^*(\hat{\mathbf{p}}) \Psi_{JJ_z}^{1, L, S}(E_1), \end{aligned} \quad (31)$$

where \mathbf{p} is the c.m. relative momentum between proton and ${}^3\text{H}$ in the final state, $E_1 = p^2/2\mu_1$, μ_1 being the $p + {}^3\text{H}$ reduced mass, σ_L is the Coulomb phase shift, and $\Psi_{JJ_z}^{1,L,S}(E_1)$ the scattering wave function given in Eq. (23). Note that in this subsection, the dependence on JJ_z is explicitly reported. Now, as discussed above, we can reduce the calculation considering only the product $H^0\ell_0$ and the contribution of the wave with $J = L = S = 0$. Therefore

$$\begin{aligned} H^0 &= \langle \Psi_{m_3, m_1}^{1+3}(\mathbf{p}) | \hat{\rho}(\mathbf{q}) | \Psi_0 \rangle , \\ &\approx \sqrt{4\pi} \left(\frac{1}{2}, m_3, \frac{1}{2}, m_1 | 0, 0 \right) e^{i\sigma_0} \langle \Psi_{0,0}^{1,0,0}(E_1) | \hat{\rho}(\mathbf{q}) | \Psi_0 \rangle \\ &= \sqrt{4\pi} \left(\frac{1}{2}, m_3, \frac{1}{2}, m_1 | 0, 0 \right) e^{i\sigma_0} \sqrt{4\pi} C_0^{000}(q, E_1) , \end{aligned} \quad (32)$$

where Ψ_0 is the ${}^4\text{He}$ ground state wave function and $C_0^{000}(q, E_1)$ the monopole ($\ell = 0$) reduced matrix element (RME) of the charge operator, which we define as

$$\langle \Psi_{0,0}^{1,0,0} | \hat{\rho}(\mathbf{q}) | \Psi_0 \rangle = \sqrt{4\pi} C_0^{000}(q, E_1) . \quad (33)$$

Thus

$$\sum_{m_3, m_1} H^0 (H^0)^* = (4\pi)^2 |C_0^{000}(q, E_1)|^2 , \quad (34)$$

The leptonic current matrix element ℓ^μ is given by

$$\ell_{\mathbf{k}s, \mathbf{k}'s'}^\mu = \bar{u}(\mathbf{k}', s') \gamma^\mu u(\mathbf{k}, s) , \quad (35)$$

where we have chosen to normalize the four spinors as $u^\dagger u = 1$. Clearly, we have to consider only ℓ^0 . The sum over the electron spins can be now obtained easily

$$\sum_{s, s'} \ell^0 (\ell^0)^* = 1 + \cos \theta , \quad (36)$$

where $\cos \theta = \hat{k} \cdot \hat{k}'$ and θ is the electron scattering angle. Thus

$$\begin{aligned} d\sigma &= \frac{1}{2} \sum_{\mathbf{k}', \mathbf{p}_1, \mathbf{p}_3} \left(\frac{4\pi\alpha}{Q^2} \right)^2 (4\pi)^2 |C_0^{000}(q, E_1)|^2 (1 + \cos \theta) \\ &\quad \times \delta \left(k + M_4 - k' - M - M_3 - \frac{p_1^2}{2M} - \frac{p_3^2}{2M_3} \right) \delta_{\mathbf{q}, \mathbf{p}_1 + \mathbf{p}_3} . \end{aligned} \quad (37)$$

The total momentum of the two nuclear clusters is $\mathbf{P} = \mathbf{p}_1 + \mathbf{p}_3$, while the relative momentum is $\mathbf{p} = (M\mathbf{p}_3 - M_3\mathbf{p}_1)/(M + M_3)$. Clearly, $\sum_{\mathbf{p}_1, \mathbf{p}_3} \equiv \sum_{\mathbf{P}, \mathbf{p}}$ and

$$\frac{p_1^2}{2M} + \frac{p_3^2}{2M_3} = \frac{p^2}{2\mu_1} + \frac{P^2}{2(M + M_3)} \equiv E_1 + \frac{P^2}{2(M + M_3)} . \quad (38)$$

The momentum-conserving delta function fixes $\mathbf{P} = \mathbf{q}$. At this point we can go to the continuum limit and write

$$\sum_{\mathbf{k}', \mathbf{p}} = \int \frac{d^3 k'}{(2\pi)^3} \frac{d^3 p}{(2\pi)^3} . \quad (39)$$

However, we will not integrate over the momentum direction of the outgoing electron since we want to compute the differential cross section $d\sigma/d\hat{k}' \equiv d\sigma/d\Omega$. The modulus of \mathbf{k}' is fixed by the energy-conservation delta. We have

$$\int dk' \delta\left(k - \Delta B - k' - \frac{q^2}{2(M + M_3)}\right) F(k') = f_R F(k')|_{k'=k-\Delta B+\dots} , \quad (40)$$

where

$$f_R = \frac{1}{1 + \frac{k' - k \cos \theta}{(M + M_3)}} , \quad \Delta B = E_1 + M + M_3 - M_4 \approx 20 \text{ MeV} . \quad (41)$$

The ‘‘recoil’’ factor f_R can be safely approximated to 1. For example, in the MAMI experiment we have $k = 795$ MeV (in the worst case) and the outgoing detector is placed at an angle of $\theta = 18, 3^\circ$. Since $k' \approx k$, f_R turns out to be ≈ 0.99 . So in the following we will take simply $f_R = 1$. Moreover $Q^2 = (\mathbf{k}' - \mathbf{k}')^2 - (k - k')^2 = 4kk' \sin^2(\theta/2)$. Putting all together, we obtain

$$\begin{aligned} \frac{d\sigma}{d\Omega} &\approx \frac{1}{2} \int \frac{d^3 p}{(2\pi)^3} \frac{dk' k'^2}{(2\pi)^3} \left(\frac{4\pi\alpha}{Q^2}\right)^2 (4\pi)^2 |C_0^{000}(q, E_1)|^2 (1 + \cos \theta) \\ &\quad \times 2\pi \delta\left(k - \Delta B - k' - \frac{q^2}{2(M + M_3)}\right) , \end{aligned} \quad (42)$$

$$= \frac{4}{\pi} \frac{\alpha^2}{Q^4} k'^2 (1 + \cos \theta) \int d^3 p |C_0^{000}(q, E_1)|^2 , \quad (43)$$

$$= \frac{\alpha^2}{4k^2 \sin^4(\theta/2)} \cos^2(\theta/2) \int_0^\infty dE_1 8\mu_1 p |C_0^{000}(q, E_1)|^2 , \quad (44)$$

$$= \left(\frac{d\sigma}{d\Omega}\right)_{Mott} \int_0^\infty dE_1 8\mu_1 p |C_0^{000}(q, E_1)|^2 . \quad (45)$$

We remember that $p = \sqrt{2\mu_1 E_1}$ and $k' = k - \Delta B + \dots$. Above, $\frac{d\sigma}{d\Omega}_{Mott}$ is the Mott cross section, i.e. the differential cross section for the scattering of an electron by a point-like charge.

As in the experiment, we define

$$|F_M(q)|^2 = \frac{d\sigma}{d\Omega} / \left[Z^2 4\pi \left(\frac{d\sigma}{d\Omega}\right)_{Mott} \right] . \quad (46)$$

Here $Z = 2$ takes into account the total charge of the ${}^4\text{He}$ nucleus. Finally

$$|F_M(q)|^2 = \frac{1}{16\pi} \int_0^\infty dE_1 \, 8p\mu_1 |C_0^{000}(q, E_1)|^2. \quad (47)$$

This expression is correct up to the $n + {}^3\text{He}$ threshold. Above, it has to be modified as

$$|F_M(q)|^2 = \frac{1}{16\pi} \sum_{\gamma=1,2} \int_0^\infty dE_\gamma \, 8p_\gamma\mu_\gamma |C_0^{000}(q, E_\gamma)|^2, \quad (48)$$

where $p_\gamma = \sqrt{2\mu_\gamma E_\gamma}$, μ_γ is the reduced mass for the clusterization γ , and $C_0^{000}(q, E_\gamma)$ the RME coming from $\langle \Psi_{0,0}^{\gamma,0,0}(E_\gamma) | \hat{\rho}(\mathbf{q}) | \Psi_0 \rangle$. The expression given in Eq. (47) agrees with those used in Ref. [9] (where the sum over the final states was obtained using the LIT), as discussed in Appendix A.

3 Results

First of all, we compute the scattering wave functions $\Psi_{0,0}^{\gamma,0,0}(E_\gamma)$ for various center-of-mass (c.m.) energy E_γ . The calculation has been performed by increasing the size of the HH basis as discussed before. As an example, we report the results for the $p + {}^3\text{H}$ phase-shift calculated at $E_1 = 0.20, 0.55, 0.74$, and 1.50 MeV in Table 2. The calculations have been performed with the N3LO500/N2LO500 and N3LO600/N2LO600 NN+3N chiral interactions. As it can be seen, the convergence is quite slow especially at the lowest energy, namely close to the resonance position. As the energy is increased, the convergence is faster. At $E = 1.50$ MeV (above the opening of the $n + {}^3\text{He}$ channel), the convergence is almost achieved. In the last line of the table, the extrapolated value for the phase-shift as obtained from the calculated values for the different basis set is also reported (see Appendix B for more details about the extrapolation procedure).

In Fig. 1, we report the “extrapolated” phase-shifts calculated with both interactions, compared with the available “experimental” results, extracted from an R-matrix analysis performed in Ref. [37]. Below the $n + {}^3\text{He}$ threshold, the phase shifts show the typical resonance behavior: a sharp increase with the phase shift reaching the value 90 deg. The convergence pattern is similar for both interactions. The position of the resonance can be deduced by looking to the so-called time delay, namely the quantity $\delta'(E_1) = d\delta(E_1)/dE_1$. The energy E_R of the resonance is deduced for the energy E_1 where $\delta'(E_1)$ has a maximum and its width Γ by the value of $2/\delta'(E_R)$. In the present case, we obtain $E_R \approx 0.1$ MeV and $\Gamma \approx 0.4$ MeV.

By inspecting Fig. 1, it can be noticed that above the $n + {}^3\text{He}$ threshold there is a sharp change, since the phase shift starts to decrease steadily. This behavior is also observed in the “experimental” phase shifts. Above the $n + {}^3\text{He}$ threshold, evidently the dynamics of the reaction changes. In fact, the process $p + {}^3\text{H} \rightarrow n + {}^3\text{He}$ starts to become rapidly dominant, and the reaction does not show any sign of the production of the resonant state.

Using the so determined wave functions, we can calculate the matrix elements with the ${}^4\text{He}$ ground state wave function using Eq. (32). In Fig. 2, we report the function

Table 2 Convergence of the $p + {}^3\text{H}$ phase-shift (deg) calculated at four different energies E_1 , for the three different basis sets specified in Table 1. The calculations have been performed with the N3LO500/N2LO500 and N3LO600/N2LO600 interactions. At $E_1 = 0.74$ MeV ($E_1 = 0.73$ MeV) for N3LO500/N2LO500 (N3LO600/N2LO600), we are just below the $n + {}^3\text{He}$ threshold. In the lines labeled “Extr.”, the extrapolated values for the phase shifts are reported.

basis set	N3LO500/N2LO500			
	$E_1 = 0.20$ MeV	$E_1 = 0.55$ MeV	$E_1 = 0.74$ MeV	$E_1 = 1.50$ MeV
B1	46.0	82.2	100.2	86.6
B2	46.7	82.6	100.4	86.8
B3	47.3	82.8	100.5	86.9
Extr.	49.2	83.6	101.0	87.2
basis set	N3LO600/N2LO600			
	$E_1 = 0.20$ MeV	$E_1 = 0.55$ MeV	$E_1 = 0.73$ MeV	$E_1 = 1.50$ MeV
B1	31.4	70.3	91.0	82.1
B2	32.0	70.9	91.4	82.2
B3	32.5	71.4	91.7	82.3
Extr.	34.5	73.2	92.9	82.6

$S(q, E_1) = \sum_{\gamma=1,2} 8p\mu_\gamma |C_0^{000}(q, E_\gamma)|^2$ vs E_1 calculated with the N3LO500/N2LO500 interaction (we remember that E_1 and E_2 are related by Eq. (17)). Clearly, for $E_1 < E_{thr}$, where E_{thr} is the energy where the $n + {}^3\text{He}$ channel opens, $S(q, E_1) = 8p\mu_1 |C_0^{000}(q, E_1)|^2$.

By inspecting Fig. 2, first of all, we can note the good convergence reached by this quantity as the basis sets used to describe the wave functions are enlarged. In fact, the results are very independent on the basis set A1, A2, or A3 used to describe the ground state wave function. Regarding the scattering wave functions, $S(q, E_1)$ comes out to be practically the same using basis sets B2 and B3.

Second, we note that $S(q, E_1)$ has a form of a peak, related to the formation of the 0_1^+ state in the scattering process. However, above E_{thr} , the energy dependence of $S(q, E_1)$ becomes totally different. For such energies, the process is dominated by the direct charge-exchange reaction $p + {}^3\text{H} \rightarrow n + {}^3\text{He}$, and the dynamics is not anymore related to the excitation of the 0_1^+ state. We have then adopted the following procedure.

1. We have fitted the calculated $S(q, E_1)$ for $0 < E_1 < E_{thr}$ with the function $aE_1^2 e^{-bE_1}$, determining the parameters a and b using a least-square method.
2. We have modified Eq. (47) as

$$\begin{aligned}
 |F_M(q)|^2 &= \frac{1}{16\pi} \left[\int_0^{E_{thr}} dE_1 S(q, E_1) + \int_{E_{thr}}^\infty dE_1 aE_1^2 e^{-bE_1} \right], \\
 &= \frac{1}{16\pi} \left[\int_0^{E_{thr}} dE_1 S(q, E_1) + \frac{a}{b^3} (2 + bE_{thr}(2 + bE_{thr})) e^{-bE_{thr}} \right] \quad (49)
 \end{aligned}$$

In Fig. 3, we show an example of the fit, plotting the function $\ln(S(q, E_1)/E_1^2)$. As it can be seen, for $E_1 > 0.20$ MeV the calculated values of this function are located in a

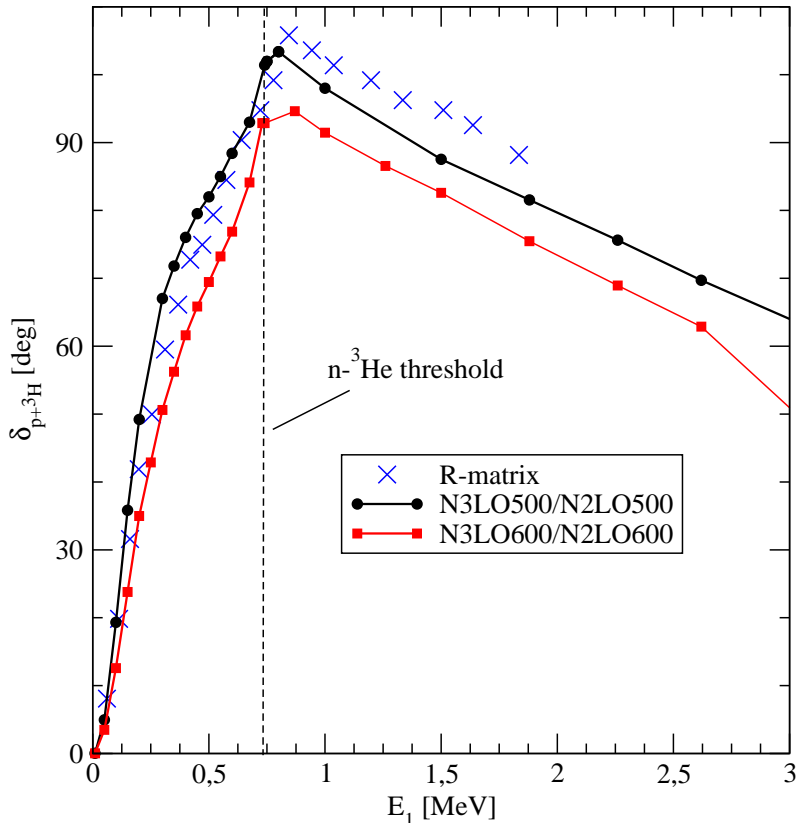


Fig. 1 (color online) $0^+ p + {}^3\text{H}$ phase shift as function of the c.m. kinetic energy E_1 calculated with the NN+3N N3LO500/N2LO500 (black curve) and N3LO600/N2LO600 (red curve) interactions. Crosses: phase-shift extracted from the R-matrix analysis [37]. The vertical dashed line denotes the energy of the $n + {}^3\text{He}$ threshold.

very good approximation along a line, easily fitted by the chosen function $\ln(a) - bE_1$. We have then prolonged $S(q, E_1)$ above E_{thr} with the simple function $aE_1^2 e^{-bE_1}$. In Fig. 4, we report the functions $S(q, E_1)$ as in Fig. 2, but for $E_1 > E_{thr}$ they are continued with the results of the fit (thin lines for $E_1 > E_{thr}$). The contribution of the $E_1 > E_{thr}$ region to the integral turns out to be about 10%. At the end, $|F_M(q)|^2$ is calculated using solely $S(q, E_1)$ determined for $E_1 < E_{thr}$.

The result of Eq. (49) is reported in Fig. 5, for the two adopted interactions, including only the leading order (or impulse approximation) contribution. The calculations are compared with the experimental data of Refs. [4–7] and with some of the theoretical values reported in the literature [8, 9]. As it can be seen, in this case the calculations are in reasonable agreement with the experimental data, in particular with the MAMI data [7]. The spread between the calculations obtained with the N3LO500/N2LO500 and N3LO600/N2LO600, related to the different cutoff values used to regularize the potentials, reflects our current ignorance about the short-range part of the nuclear interaction.

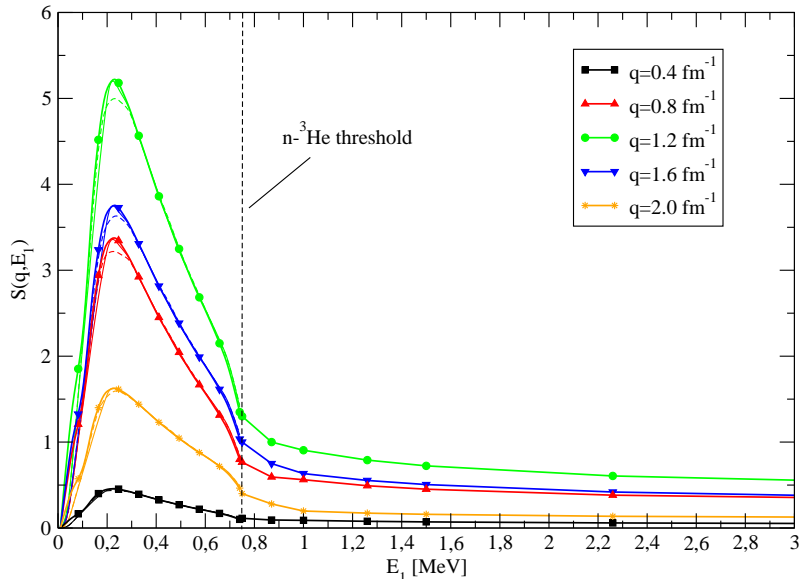


Fig. 2 (color online) The function $S(q, E_1)$ calculated for various values of q and with the N3LO500/N2LO500 interaction as function of the c.m. kinetic energy E_1 of the $p + {}^3\text{H}$ clusters. The vertical line denotes the opening of the $n + {}^3\text{He}$ channel. For each value of q , the dashed, thin solid, and thick solid lines are obtained using the sets B1, B2, and B3 in the expansion of the scattering wave function, respectively. The calculations with set B2 are practically coincident with the results obtained with set B3 and they can be hardly distinguished. Above the $n + {}^3\text{He}$ threshold only the calculations with set B3 are reported, as the results obtained with sets B1 and B2 are practically coincident. Furthermore, the results are very independent on the basis set A1, A2, or A3 used to describe the ground state wave function.

Finally, in Fig. 6, we report a calculation where the corrections beyond the leading order term for the nuclear charge operator (the relativistic corrections and meson-exchange terms) are included (“full” calculation). As it can be seen, the “full” calculations slightly reduces the monopole form factor, especially for large values of q , bringing the calculations very close to the MAMI data.

4 Conclusion

In this paper, we have studied the ${}^4\text{He}$ monopole form factor by calculating the ${}^4\text{He}(e, e'p){}^3\text{H}$ and ${}^4\text{He}(e, e', n){}^3\text{He}$ cross sections. The monopole form factor (squared) is then defined by the ratio of this cross section with the Mott cross section. This procedure requires the summation over all possible final energies. However, above the opening of the $n + {}^3\text{He}$ threshold, the dynamics of the process appears to drastically change, not involving anymore the formation of the ${}^4\text{He}$ first excited state (that in this approach enters as a resonant state). We have then calculated the response $S(q, E_1)$ up to E_{tr} , using an approximate procedure to complete the summation for $E > E_{tr}$. A similar procedure has been adopted also in the MAMI experiment [7], as the contribution of the process $0_0^+ \rightarrow 0_1^+$ has to be extracted in some way from the measured

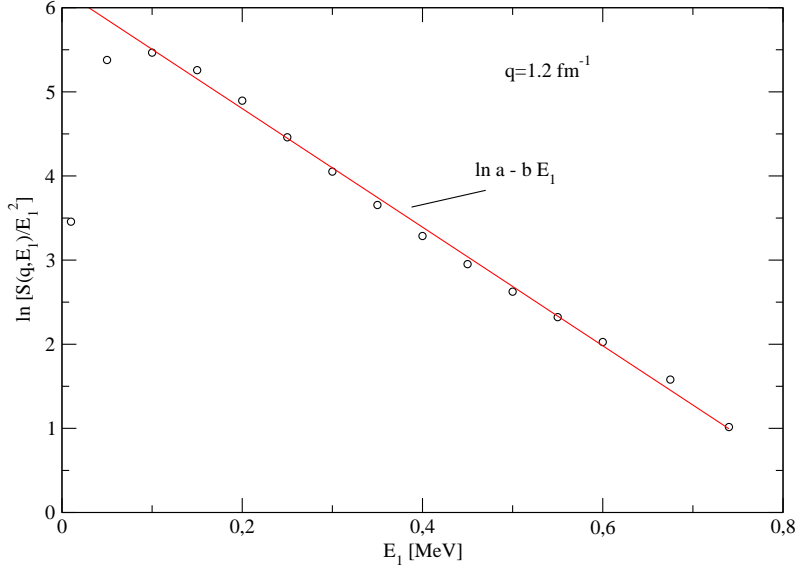


Fig. 3 (color online) Example of the fit of the calculated $S(q, E_1)$ with the function $aE_1^2 e^{-bE_1}$. Solid circles: $\ln[S(q, E_1)/E_1^2]$ calculated for $q = 1.2 \text{ fm}^{-1}$ with the N3LO500/N2LO500 interaction and the set B3 of HH functions. At it can be seen, for $E_1 > 0.2 \text{ MeV}$ the calculated values of this function are located in a very good approximation along a line, which is then fitted using a least-square method using the function $\ln(a) - bE_1$.

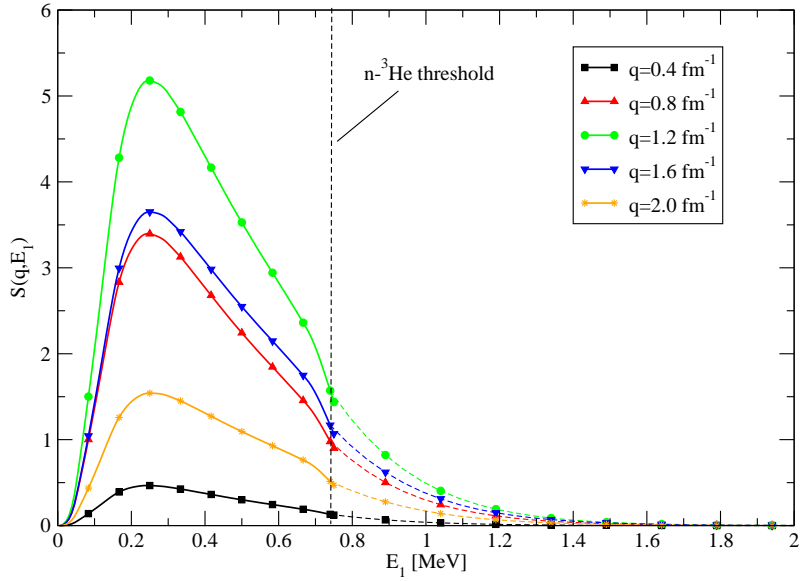


Fig. 4 (color online) The same as in Fig. 2. The dashed lines for $E_1 > E_{tr}$ show the functions $aE_1^2 e^{-bE_1}$, fitted as explained in the main text. Only the calculation of set B3 of the HH basis is shown.

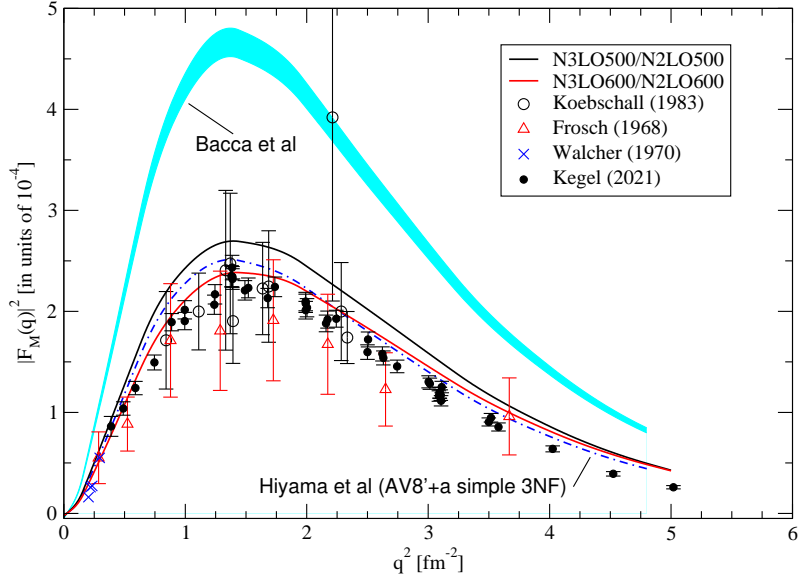


Fig. 5 (color online) The monopole form factor $|F_M(q)|^2$ calculated using Eq. (49) as function of q , obtained with the N3LO500/N2LO500 and N3LO600/N2LO600 interactions. The charge operator includes only the one-body leading-order (impulse approximation) term given in Eq. (29). The experimental data are from Refs. [4–7] The results of the calculations of Refs. [8, 9] are also reported.

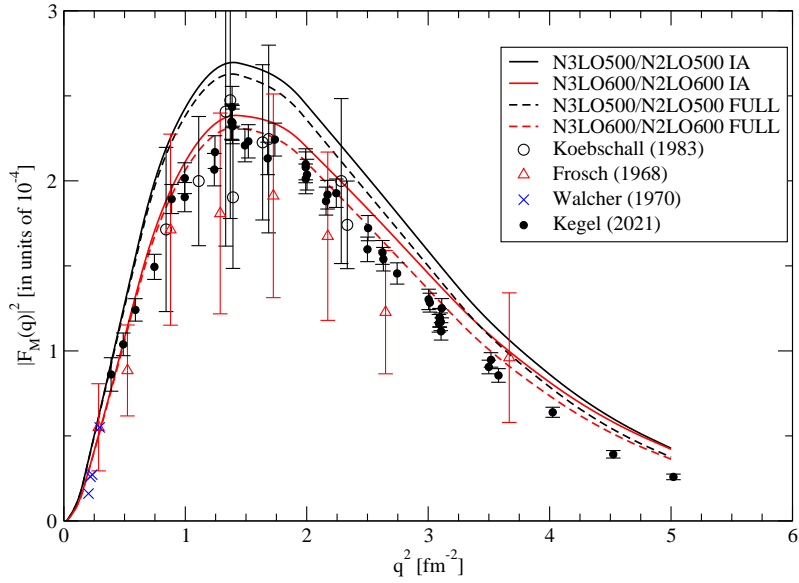


Fig. 6 (color online) The same as in Fig. 5 but adding the results obtained with the full charge operator (dashed lines), as derived in Ref. [36].

cross section of the process ${}^4\text{He}(e, e'p){}^3\text{H}$, (see Ref. [7] for the procedure adopted in the MAMI experiment).

As it can be seen by inspecting Fig. 5, our results are in reasonable agreement with the data, and with the theoretical study by Hiyama *et al.* [8] and the more recent calculations reported in Refs. [11, 12]. However, they are at variance with the calculation of Ref. [9].

Although limited to just two nuclear interaction models derived within the χEFT framework, we believe that the results obtained are significant and representative. However, it is essential to study this observable also using other interaction models. We plan to perform this study in the future, in order to better understand how the calculated $F_M(q)$ depends on the interaction.

Appendix A The formulation of Ref. [9]

In Ref. [9], the monopole form factor is defined as

$$|\tilde{F}_M(q)|^2 = \frac{1}{Z^2} \int d\omega \mathcal{S}(q, \omega), \quad (\text{A1})$$

where q, ω are as usual the momentum and energy transfer. The quantity $\mathcal{S}(q, \omega)$ is defined as

$$\mathcal{S}(q, \omega) = \sum_n |\langle n | \mathcal{M}(q) | 0 \rangle|^2 \delta(\omega - E_n + E_0). \quad (\text{A2})$$

where $|0\rangle$ and $|n\rangle$ are eigenfunctions of the the nuclear Hamiltonian, E_0 and E_n the corresponding eigenvalues, and

$$\mathcal{M}(q) = \frac{f_p(q)}{2} \sum_{j=1}^4 j_0(qr_j), \quad (\text{A3})$$

is the isoscalar monopole operator (j_0 is a Bessel function). Note that this operator is the $\ell = 0$ isoscalar component of our operator $\hat{\rho}(\mathbf{q})$ given in Eq. (29). In our case $|0\rangle$ is the ${}^4\text{He}$ ground state and $|n\rangle$ the $p + {}^3\text{H}$ scattering state, given in Eq. (31) (here we limit ourselves to consider states below the $n + {}^3\text{He}$ threshold). Considering only the contribution of the $L = S = J = 0$ wave, we have

$$\begin{aligned} \mathcal{S}(q, \omega) = & \sum_{m_1, m_3, \mathbf{p}} \left(\frac{1}{2}, m_3, \frac{1}{2}, m_1 | 0, 0\right)^2 4\pi |\langle \Psi_{0,0}^{1,0,0} | \mathcal{M}(q) | \Psi_0 \rangle|^2 \\ & \times \delta\left(\omega - M - M_3 - \frac{p^2}{2\mu_1} + M_4\right), \end{aligned} \quad (\text{A4})$$

where, as in subsection 2.3, we can neglect the recoil term $\frac{q^2}{2(M+M_3)}$ in the δ -function. Introducing the RME as in Eq. (33) and changing $\sum_{\mathbf{p}} \rightarrow \int d^3p / (2\pi)^3$, we have

$$\mathcal{S}(q, \omega) = \int \frac{d^3p}{(2\pi)^3} (4\pi)^2 |C_0^{000}(q, E_1)|^2 \delta\left(\omega - M - M_3 - \frac{p^2}{2\mu_1} + M_4\right). \quad (\text{A5})$$

The integration over $d\hat{p}$ gives simply 4π , and changing integration variable to $E_1 = \frac{p^2}{2\mu_1}$, we obtain

$$\mathcal{S}(q, \omega) = \int dE_1 8p\mu_1 |C_0^{000}(q, E_1)|^2 \delta(\omega - M - M_3 - \frac{p^2}{2\mu_1} + M_4). \quad (\text{A6})$$

Finally, by integrating over ω , we have

$$|\tilde{F}_M(q)|^2 = \frac{1}{4} \int dE_1 8p\mu_1 |C_0^{000}(q, E_1)|^2. \quad (\text{A7})$$

Note that in Ref. [9], the monopole form factor which is compared with the data is $|\tilde{F}_M(q)|^2/4\pi$, which therefore agrees with our definition of $|F_M(q)|^2$ given in Eq. (47).

Appendix B The extrapolation procedure

In this appendix, we present the procedure adopted to extrapolate a given quantity X (for example, the $p - {}^3\text{H}$ phase-shift δ , etc.) estimating the “missing” part caused by the truncation of the HH basis in the calculations. First of all, we perform several calculations of X using different basis sets $n = 0, \dots, N$ of HH functions (usually, $N = 6$). Basis set $n = 0$ is characterized by a given choice of the grand angular quantum numbers $K_\alpha^{(0)}$ for each class $\alpha = 1, \dots, 5$. Then, for the basis set n , $K_\alpha = K_\alpha^{(0)} + 2n$, etc. Let us denote with X_n the quantity X calculated with the basis set n . We have found that the ratios

$$x_n = \frac{X_n - X_{n-1}}{X_{n-1} - X_{n-2}}, \quad n = 2, \dots, N, \quad (\text{B8})$$

are, in a good approximation, independent of n . Namely, $x_n \approx x$, and x is always less than 1. That means, that each time the K_α are increased by 2, the “increment” of X is reduced by a factor x . Therefore, assuming that this property is maintained also for $n > N$, we can extrapolate the final value X_∞ of X for an “infinite” basis, as

$$X_\infty = X_N + x\Delta + x^2\Delta + x^3\Delta + \dots = X_N + \frac{x}{1-x}\Delta, \quad (\text{B9})$$

where $\Delta = X_N - X_{N-1}$. Typical values of x are around 0.8. In Table B1, we report an example of this procedure. Finally, we estimate the “error” of X_∞ by varying x by $\pm 2.5\%$.

Acknowledgements. The Authors would like to acknowledge S. Bacca, N. Barnea, W. Leidemann, and G. Orlandini for useful discussions.

References

- [1] D.R. Tilley, H.R. Weller, and G.M. Hale, Nucl. Phys. **A541**, 1 (1992)
- [2] M. Gattobigio and A. Kievsky, Few-Body Syst. **64**, 86 (2023)

Table B1 Convergence of the $p + {}^3\text{H}$ phase-shift δ at $E_1 = 0.20$ MeV, calculated with the N3LO500/N2LO500 interaction, using basis set n . In the third column, the ratio $x_n = (X_n - X_{n-1})/(X_{n-1} - X_{n-2})$ is given. In the last row, we report the extrapolated values of δ using Eq. (B9), with $x = x_6$.

Basis set n	$p + {}^3\text{H}$ scattering at $E_1 = 0.20$ MeV δ_n (deg)	x_n
0	40.10	—
1	42.20	—
2	43.83	0.78
3	45.04	0.74
4	45.98	0.78
5	46.70	0.77
6	47.26	0.78
Extr.	49.24	

- [3] E. Epelbaum, Physics **16** 58 (2023)
- [4] Th. Walcher, Phys. Lett. **B31**, 442 (1970)
- [5] R.F. Frosch *et al.*, Nucl. Phys. **A110**, 657 (1968)
- [6] G. Kobschall *et al.*, Nucl. Phys. **A405**, 648 (1983)
- [7] S. Kegel *et al.*, Phys. Rev. Lett. **130**, 152502 (2023)
- [8] E. Hiyama, B.F. Gibson, and M. Kamimura, Phys. Rev. C **70**, 031001(R) (2004)
- [9] S. Bacca, N. Barnea, W. Leidemann, and G. Orlandini, Phys. Rev. Lett. **110**, 042503 (2013)
- [10] S. Bacca, N. Barnea, W. Leidemann, and G. Orlandini, Phys. Rev. C **91**, 024303 (2015)
- [11] N. Michel, W. Nazarewicz and M. Ploszajczak, [arXiv:2306.05192](https://arxiv.org/abs/2306.05192)
- [12] Ulf-G. Meißner, S. Shen, S. Elhatisari, and D. Lee, [arXiv:2309.01558](https://arxiv.org/abs/2309.01558)
- [13] S. Bogner, T. Kuo, and A. Schwenk, Physics Reports **386**, 1 (2003)
- [14] R.B. Wiringa, V.G.J. Stoks, and R. Schiavilla, Phys. Rev. C **51**, 38 (1995)
- [15] D.R. Entem and R. Machleidt, Phys. Rev. C **68**, 041001(R) (2003)
- [16] R. Machleidt and D.R. Entem, Phys. Rep. **503**, 1 (2011)
- [17] E. Epelbaum *et al.*, Phys. Rev. C **66**, 064001 (2002)

- [18] P. Navrátil, *Few-Body Syst.* **41**, 117 (2007)
- [19] A. Gardestig and D.R. Phillips, *Phys. Rev. Lett.* **96**, 232301 (2006)
- [20] D. Gazit, S. Quaglioni, and P. Navrátil, *Phys. Rev. Lett.* **103**, 102502 (2009)
- [21] L.E. Marcucci, A. Kievsky, S. Rosati, R. Schiavilla, and M. Viviani, *Phys. Rev. Lett.* **108**, 052502 (2012); *Erratum*, *Phys. Rev. Lett.* **121**, 049901(E) (2018)
- [22] A. Baroni *et al.*, *Phys. Rev. C* **98**, 044003 (2018)
- [23] L. E. Marcucci, F. Sammarruca, M. Viviani, and R. Machleidt, *Phys. Rev. C* **99**, 034003 (2019)
- [24] A. Kievsky *et al.*, *J. Phys. G: Nucl. Part. Phys.* **35**, 063101 (2008)
- [25] L. E. Marcucci *et al.*, [ArXiv:1912.09751](https://arxiv.org/abs/1912.09751)
- [26] H. Kamada, A. Nogga, W. Glockle, E. Hiyama, M. Kamimura, K. Varga, *et al.*, *Phys. Rev. C* **64**, 044001 (2001)
- [27] M. Viviani, A. Kievsky, and S. Rosati, *Phys. Rev. C* **71**, 024006 (2005)
- [28] M. Viviani, A. Deltuva, R. Lazauskas, J. Carbonell, A.C. Fonseca, A. Kievsky, L.E. Marcucci, and S. Rosati, *Phys. Rev. C* **84**, 054010 (2011)
- [29] M. Viviani, A. Deltuva, R. Lazauskas, A. C. Fonseca, A. Kievsky, and L. E. Marcucci, *Phys. Rev. C* **95**, 034003 (2017)
- [30] M. Viviani, L. Girlanda, A. Kievsky, and L.E. Marcucci, *Phys. Rev. C* **102**, 034007 (2020)
- [31] F. Zernike and H.C. Brinkman, *Proc. Kon. Ned. Acad. Wensch.* **33**, 3 (1935)
- [32] M. Fabre de la Ripelle, *Ann. Phys. (N.Y.)* **147**, 281 (1983)
- [33] M. Abramowitz and I. Stegun, *Handbook of Mathematical Functions* (Dover Publications, Inc., New York, 1970)
- [34] A. Nogga, A. Kievsky, H. Kamada, W. Glockle, L.E. Marcucci, S. Rosati, and M. Viviani, *Phys. Rev. C* **67**, 034004 (2003)
- [35] G. Shen, L. E. Marcucci, J. Carlson, S. Gandolfi, and R. Schiavilla *Phys. Rev. C* **86**, 035503 (2012)
- [36] S. Pastore, L. Girlanda, R. Schiavilla, and M. Viviani, *Phys. Rev. C* **84**, 024001 (2011)
- [37] H.M. Hofmann and G.M. Hale, *Phys. Rev. C* **77**, 044002 (2008)